Progress In Electromagnetics Research M, Vol. 6, 91–105, 2009

ON THE RADIATION PATTERN OF THE L-SHAPED WIRE ANTENNA

A. Andújar, J. Anguera, and C. Puente †

Technology and Intellectual Property Rights Department
Fractus
Barcelona, Spain

A. Pérez

Electronics and Communications Department
Universitat Ramon Llull
Barcelona, Spain

Abstract—An objective of the present study is to make a physical insight into the radiation properties of an L-shaped wire antenna. More specifically, the study is focused on the effects of the antenna geometry over the characteristic radiation pattern of an L-shaped wire antenna. Regarding the basic equations for the radiated field, three main regions according to the length-height ratio of an L-shaped wire antenna have been determined. The said regions depict the geometrical boundaries where the L-shaped wire antenna loses its characteristic monopole-type radiation pattern. In this sense and relating to the aspect ratio of the L-shaped antenna, the said radiation properties can be easily varied in order to achieve a half isotropic radiation pattern or even, a patch-type radiation pattern. Thus, the method described herein demonstrates that simple modifications applied to the geometry of a basic structure, allow obtaining radiation properties associated to more complex structures.

Corresponding author: J. Anguera (jaume.anguera@fractus.com).
† J. Anguera is also with Electronics and Communications Department, Universitat Ramon Llull, Barcelona, Spain; C. Puente is also with Signal Theory and Communications, Universitat Politècnica de Catalunya, Barcelona, Spain.

1. INTRODUCTION

The L-shaped wire antenna is a structure that has been extensively analyzed in the literature. The efforts have mainly been focused on determining the input impedance of an inverted L-monopole, shown in [1]. In the same manner, a simplified equivalent circuit of a ?/4 transmission line antenna is proposed in [2] to determine the input impedance and the current distributions of the structure. An L-monopole antenna can also be associated to the well-known top-loaded antennas seen in [3], where the input impedance and the current distribution of this kind of structures are analyzed. However, no mention about its radiation properties is made. At the same time, as in [4] it is possible to determine the effects of bending the $\lambda/4$ transmission line antenna over the radiation pattern. This action provides a short dipole-type radiation pattern featured by a toroid shape. Nevertheless, the study of the far-field equations is carried out always assuming a length of $\lambda/4$. In addition, simple analytic methods have been proved to be very useful for determining radiation pattern of wire antennas, as seen in [5], which concentrates on the effects produced by the proximity of a high impedance material over several antenna properties, such as impedance, gain and radiation pattern. Other analytic methods have been used to determine the current distribution for wire antennas above lossy spaces [6].

All studied references in the literature, which analyze the current distribution and the electrical fields, take only into account a $\lambda/4$ length, which is the length where the antenna produces a monopole-type radiation pattern [7]. As a consequence, this study proposes a simple method to easily determine the radiation pattern properties of an L-shaped wire antenna, by just knowing the ratio between the length associated to the horizontal arm (hereafter L_x) and the height of the vertical arm (hereafter h) (see Fig. 1). This proposal provides an important degree of freedom, since by just modifying this ratio it is possible to obtain a monopole-type, a half-isotropic-type or even a patch-type radiation pattern.

The structure of this paper is organized as follows. Firstly, a theoretical study regarding the image theory concept is presented in Section 2. The influence of the antenna geometry over the radiation properties of the antenna becomes evident in this section. In Section 3, regarding the theoretical study, the conditions needed to achieve a monopole-type, a half-isotropic type, or even a patch-type radiation pattern are determined. Subsequently, the L-shaped wire antenna is designed and simulated with the IE3D software. The results that corroborate the effectiveness of the proposed method are shown in

Section 4. Finally, the conclusions are presented in Section 5.

2. BASIC THEORY

The antenna under study is a basic L-shaped wire antenna consisting of two radiating arms. The horizontal radiating arm is featured by the variable length L_x, whereas the vertical radiating arm is characterized by the variable height h. The antenna is located in the x-z plane over a Perfect Electrical Conductor (PEC) and the feeding point is placed at the coordinates origin ($x = y = z = 0$), as Fig. 1 depicts.

The radiation of an L-shaped wire antenna can be divided into two parts, one due to the vertical arm and the other due to the horizontal arm. Applying image-theory [8], the radiation equations may be derived.

Figure 1(a) shows the vertical arm, which is mainly responsible for the monopole-type radiation pattern. On the contrary, Fig. 1(b) depicts the horizontal arm, which produces a patch-type radiation pattern. By superposition, it is possible to state that the radiation pattern associated to the L-shaped wire antenna (shown in Fig. 1(c)) is an addition of the individual radiation patterns of each arm that compose the L-shaped wire antenna.

As aforementioned, the combination of these components forms the L-shaped wire antenna structure (shown in Fig. 1(c)), and the ratio between h and L_x defines the contribution of each one of said radiating arms to the radiation pattern of the L-shaped antenna structure. A basic mathematical analysis following the image theory has been carried out in order to obtain the radiated far-field equations as a function of h and L_x according to [8].

On one hand, the Equation (1) highlights the relevance of the current distribution over the electrical field value in both components, *E-theta* (hereafter E_θ) and *E-phi* (hereafter E_φ). Nevertheless, while the component E_θ is dependant of the current distribution of both radiating arms (I_1 and I_2), the E_φ component is only affected by the current distribution of the horizontal radiating arm, I_2 (the vertical arm does not radiate an E_φ field).

$$\begin{aligned} E_\theta &= -j30\frac{e^{-jkr}}{r}\left(I_2\cos\theta\frac{e^{jk_x\frac{L_x}{2}}}{\sin\theta}\sin\left(k_x\frac{L_x}{2}\right)4j\sin\left(k_zh\right)-I_1\sin\theta\frac{2\sin\left(k_zh\right)}{\cos\theta}\right) \\ E_\varphi &= -j30\frac{e^{-jkr}}{r}\left(-I_2\sin\varphi\frac{e^{jk_x\frac{L_x}{2}}}{\sin\theta\cos\varphi}\sin\left(k_x\frac{L_x}{2}\right)4j\sin\left(k_zh\right)\right) \end{aligned} \quad (1)$$

L_x: is the length of the horizontal radiating arm.
h: is the height of the vertical radiating arm.

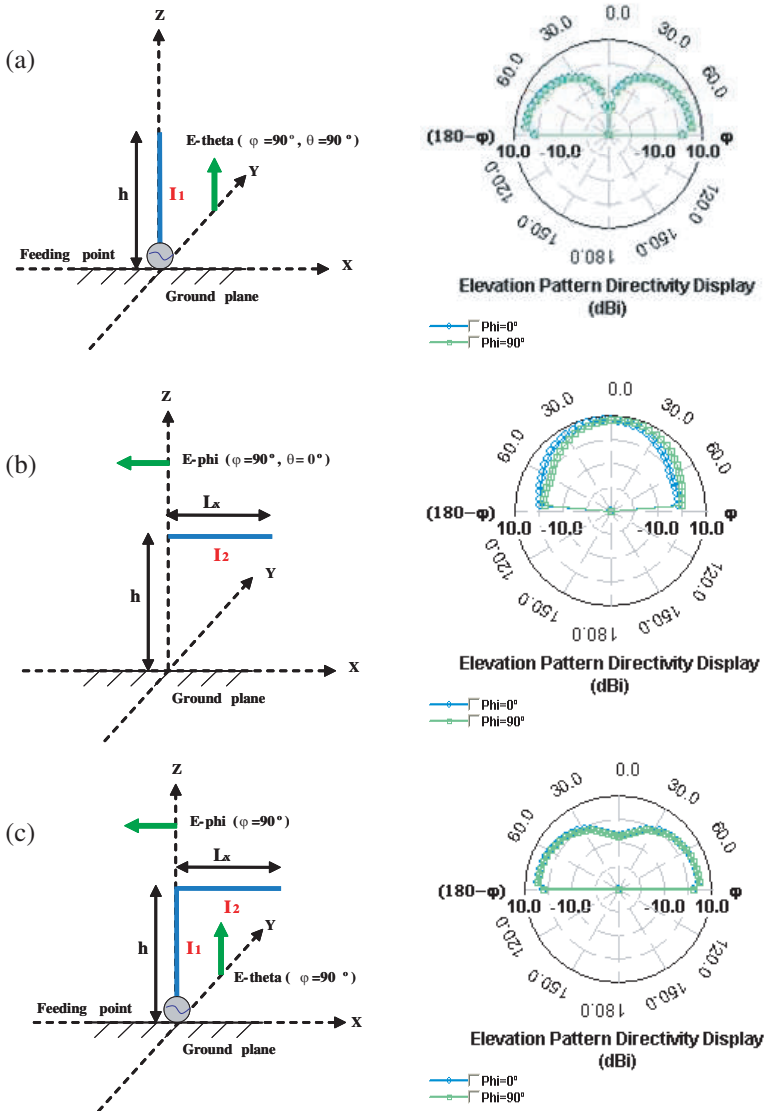

Figure 1. Decomposition of an L-shaped wire antenna in two arms and representation of the radiation pattern. (a) Vertical arm mainly responsible for the monopole-type radiation pattern; (b) Horizontal arm mainly responsible for the patch-type radiation pattern; (c) L-shaped wire antenna combining both contributions, horizontal and vertical (these radiation patterns are illustrative examples).

k_x, k_z: are the rectangular components of the k vector. It is straightforward to convert them into spherical components by means of the following equations:

$$k_x = k \sin\theta \cos\varphi \quad k_z = k \cos\theta \tag{2}$$

The equations presented in (1) allow to easily determine the electrical field value at any space coordinate, defined by θ and φ angles, and as a function of the geometry and the current distribution of the L-shaped wire antenna. Following the obtained results, the radiation pattern at any θ, φ value is determined by E_θ and E_φ, the directions of which are depicted in Fig. 1(c). Thus, the influence of both arms in the radiation is evident, which underlines the possibility of a radiation pattern reconfiguration through the manipulation of the geometry and the current distribution of the L-shaped antenna structure.

3. ANALYTIC RESULTS

Figure 1(c) depicts the location of the L-shaped wire antenna in the coordinates axes. The schematic representation shows that the radiation pattern in the $\varphi = 0^\circ$ and $\varphi = 90^\circ$ planes is a combination of E_φ and E_θ components, produced by each radiating arm.

The independent contribution of both components to the radiation gives the antenna designer an important degree of freedom. As a first approximation, the length of the elements could be adjusted in order to provide a patch-type radiation pattern, a monopole-type radiation pattern or even a half-isotropic radiation pattern. In order to achieve the desirable radiation pattern a time-consuming parametric study would be needed. However, this paper presents a simple method to determine the h to L_x ratio needed to obtain a specific radiation pattern, avoiding, in this way, the annoying trial and error method.

Consequently, the main aim of the next subsections consists in determining the ratio between E_φ at $\theta = 0^\circ$, $\varphi = 90^\circ$ (hereafter patch direction (Fig. 1(b))) and E_θ at $\theta = 90^\circ$, $\varphi = 90^\circ$ (hereafter monopole direction (Fig. 1(a))). For instance, if the field in the patch direction predominates over the field in the monopole direction, a patch-type radiation pattern would be expected.

Considering the relevance of the current distribution, this section is divided into three subsections regarding a specific current distribution. The proposal begins with the most simplified current distribution model and finishes in the most accurate approximation.

3.1. Uniform Current Distribution

In this subsection, a uniform current distribution along the wire is assumed. Hence, current values are approximated to $I_1 = I_2 = 1$. Although, this is an ideal situation, it may be achieved by loading the wire with reactive elements [9].

The results determine three main regions of operation, which are depicted in Fig. 2. The y-coordinate axis depicts the ratio between E_φ and E_θ components in the patch and monopole directions respectively, while the x-coordinate axis makes references to the total length of the L-shaped wire antenna in terms of λ, with the total length defined as the addition of L_x and h.

The E_φ component, produced by the horizontal arm is responsible for the patch-type component. As previously explained, it is calculated in the patch direction. On the contrary, the E_θ component provided by the vertical arm and featured by a monopole-type component is measured in a different direction, and more specifically, in the monopole direction. The particularization to the plane φ=90° is made for the purpose of simplifying the equations.

Thus, in the graph, a ratio equal to ± 3 dB means that no component is significantly predominant over the other. In the same way, under this condition the electrical radiated field in the patch direction is approximately equal to the electrical radiated field in the monopole direction. Consequently a half-isotropic radiation pattern is obtained. The geometrical conditions to achieve this situation are shown in Fig. 2.

In the same way, a ratio below < -3 dB means that the E_φ component is weaker than the E_θ, or likewise, the component in the patch direction is negligible in front of the electrical radiated field component in the monopole direction. This situation is also depicted in Fig. 2 and it is associated to a monopole-type radiation pattern.

Finally, higher ratio values, above $> +3$ dB, are associated to a patch-type behaviour in radiation pattern terms, since under these situations the patch direction component is stronger than the monopole direction one. The geometrical conditions needed for achieving this situation are depicted in Fig. 2. It is possible to conclude that the results obtained from the image theory analysis gathered in Fig. 2, clearly show the benefits of this study. From the graph it is really straightforward to determine the necessary length for achieving a specific radiation pattern, avoiding the well-known trial and error method. For instance, if $h/L_x = 0.5$ and $L \leq 0.05\lambda$, a monopole-type pattern is obtained, whereas for lengths between $0.05\lambda \leq L \leq 0.15\lambda$ a half-isotropic-type radiation pattern is achieved. Another interesting conclusion is that for $h/L_x = 2$, a broadband half-isotropic type

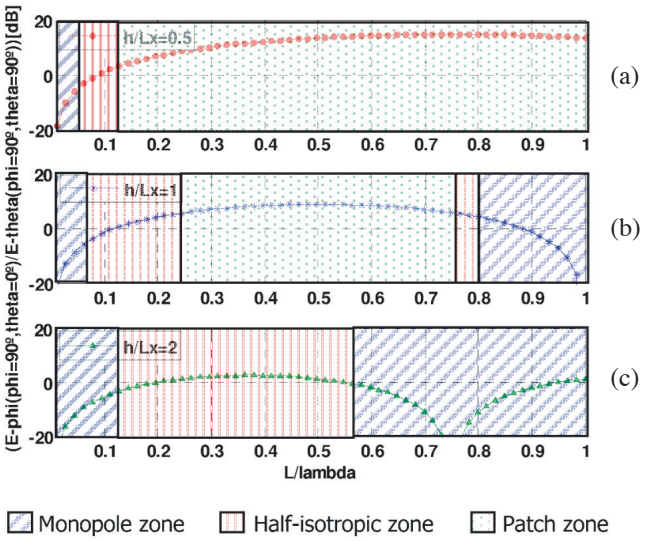

Figure 2. Ratio between component E_φ (Patch direction) and E_θ (Monopole direction) as an L_{total}/λ function, for several h/L_x values. (a) $h/L_x = 0.5$; (b) $h/L_x = 1$; (c) $h/L_x = 2$.

radiation pattern may be obtained since the ratio keeps approximately constant for $0.15\lambda \leq L \leq 0.57\lambda$. It becomes an interesting topic to research, mainly due to the fact that it depends on how uniform the current may be when the antenna is loaded with reactive elements.

As Fig. 2 shows, the properties of the curve are strongly dependant on the ratio between h and L_x. The higher the ratio between h and L_x is, the higher the range is where the L-shaped wire antenna presents a monopole-type radiation pattern. Otherwise, the lower the ratio is, the higher the range is where the antenna behaves as a patch-type, in radiation pattern terms.

Furthermore, it is necessary to remember that the curves depicted in Fig. 2 are theoretical values, since a uniform current distribution is considered. As stated before, a uniform current distribution can be obtained by loading the wire with reactive elements, for other cases, the current is not uniform but sinusoidal, which is considered in Section 3.3. For those antennas with a length smaller than 0.25λ, a better approximation closer to real situations would consider a triangular current distribution, as following subsection describes.

3.2. Triangular Current Distribution

As the schematic Fig. 3 depicts, a triangular current distribution is characterized by a maximum of current at the location of the feeding point. Fig. 3 shows an example per $h = L_x$. The current from the feeding point to the open end of the L-shaped antenna structure decreases linearly. Thus, it is straightforward to approximate the current intensity values along the vertical and the horizontal radiating arms. As Fig. 3 shows, I_1, which is the current associated to the vertical radiating arm has been calculated as an average between the intensity values along this structure. On the other hand and regarding the current intensity decrement along the structure, I_2 has been approximated in the same way. As a result, it is possible to conclude that in a triangular current distribution I_1 is always higher than I_2 and consequently, the radiated field component E_φ suffers a reduction with respect to the theoretical case where a uniform current distribution is assumed.

It is important to notice that this triangular current distribution may be only considered for unloaded L-shaped wire antennas with a total wire length lower than 0.25λ. For larger lengths, a more complex current distribution must be regarded. In this sense, only the effect of having a triangular or uniform current distribution, when $h + L_x < 0.25\lambda$, can be considered.

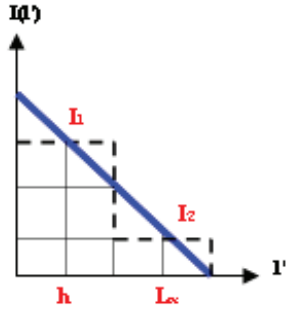

Figure 3. Schematic associated to a triangular current distribution. l' is the parameter defining the path along the wire.

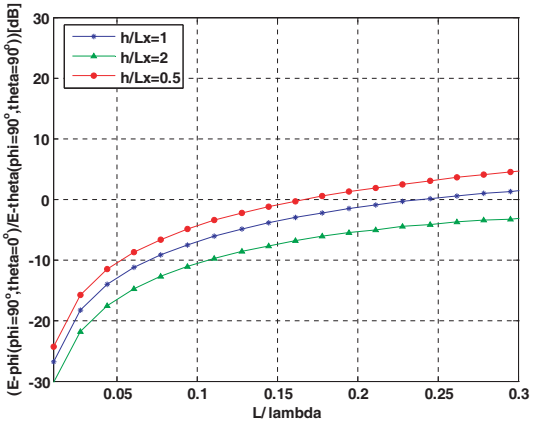

Figure 4. Ratio between component E_φ (Patch direction) and E_θ (Monopole direction) as an L/λ function, regarding a triangular current distribution. (a) $h/L_x = 1$, (b) $h/L_x = 2$, (c) $h/L_x = 0.5$.

Fig. 4 demonstrates the effect of regarding a triangular current distribution over the first approximation in Fig. 2, where a theoretical uniform current distribution was considered. The comparison is established for three cases: h/L_x=0.5, h/L_x=1 and h/L_x=2. It is possible to observe that the fact of regarding a triangular current distribution causes a displacement of the curve to lower ratio values for all the considered cases.

Consequently the areas that define the radiation pattern behaviour when a triangular current distribution is considered (Fig. 4), slightly differs from the case where a uniform current distribution is approximated (Fig. 2). If a uniform current distribution is achieved, the necessary length for obtaining a patch-type radiation pattern is reduced with respect to the situation where the current follows a triangular distribution. However, as a theoretical uniform current distribution can not be attainable in real environments without the help of reactive elements, a triangular current distribution becomes the most appropriated approximation if $h + L_x < 0.25\lambda$, and in this sense the curve associated to Fig. 4 is more practical.

As explained above, the displacement effect observed over the curve with $h/L_x = 1$ is also present for other ratios, which is depicted in Fig. 4 and shows approximately the same behaviour. This effect, in the three cases, increases the length of the L-shaped wire antenna needed to obtain a patch-type radiation pattern. However, it is interesting to remark that with length to height ratios lower than 1, such as $h/L_x = 0.5$, it is possible to obtain a patch-type radiation pattern for lengths lower than 0.25λ.

Consequently, it is possible to conclude that for short unloaded L-shaped wire antennas, the monopole-type radiation pattern is the typical behaviour.

3.3. Sinusoidal Current Distribution

Although the triangular current distribution results as a good approximation, a general case for knowing the current distribution for wire lengths higher than 0.25λ is proposed. In this case, according to [8], the sinusoidal current distribution is:

$$I\left(l'\right) = \sin\left[k\left(L - l'\right)\right] \tag{3}$$

where l' is the parameter defining the path along the wire.

Since we are interested in the $E_\varphi(\varphi = 90^\circ,\ \theta = 0^\circ)$ and $E_\theta(\varphi =$

$\theta = 90°$), the radiation equations become as follows:

$$\begin{aligned}
\vec{N}_1 &= \hat{z} \int_{-h}^{h} I_1(z') e^{jkz' \cos\theta} dz' \\
\vec{N}_{2up} &= \hat{x} \int_{0}^{L_x} I_2(x') e^{jkh\cos\theta} e^{jkx' \sin\theta \cos\varphi} dx' \\
\vec{N}_{2image} &= -\hat{x} \int_{0}^{L_x} I_2(x') e^{-jkh\cos\theta} e^{jkx' \sin\theta \cos\varphi} dx'
\end{aligned} \tag{4}$$

Where $\vec{N}_1$ is the radiation vector for the vertical arm, and $\vec{N}_{2u}, \vec{N}_{2image}$ are the radiation vectors for the horizontal arm and its image, respectively.

Transforming the radiation vector to spherical coordinates and particularizing the radiation field equations to $E_\varphi(\varphi = 90°,\ \theta = 0°)$ and $E_\theta(\varphi = \theta = 90°)$ result in:

$$\begin{aligned}
E_\theta(\varphi = \theta = 90°) &= \int_{-h}^{h} I_1(z') dz' \\
E_\varphi(\varphi = 90°,\ \theta = 0°) &= -2j \sin(kh) \int_{0}^{L_x} I_2(x') e^{jkx'} dx'
\end{aligned} \tag{5}$$

Where

$$I_1(z') = I\big(l' = z'\big), \qquad I_2(x') = I\left(l' = x' + h\right) \tag{6}$$

Equation (5) can be easily computed for several h/L_x ratios as shown in Fig. 5.

From this data, we can conclude that the $h/L_x = 2$ behaves as a monopole for a wide frequency range. However, for $h/L_x = 1$ and 0.5 the monopole behaviour as obtained for electrically short length up to 0.5λ and 0.4λ, respectively. In fact, at 0.5λ (for $h/L_x = 1$) and 0.4λ (for $h/L_x = 0.5$), the magnitude of the field in the monopole and patch directions becomes the same. This result indicates the possibility of a half-isotropic pattern. For larger lengths up to 0.7λ, the field magnitude in the patch directions is stronger than in the monopole directions indicating the possibility of a patch-type radiation pattern. To corroborate these analytic predictions, numerical simulation using MoM is used. Radiation cuts are computed and shown in the next section.

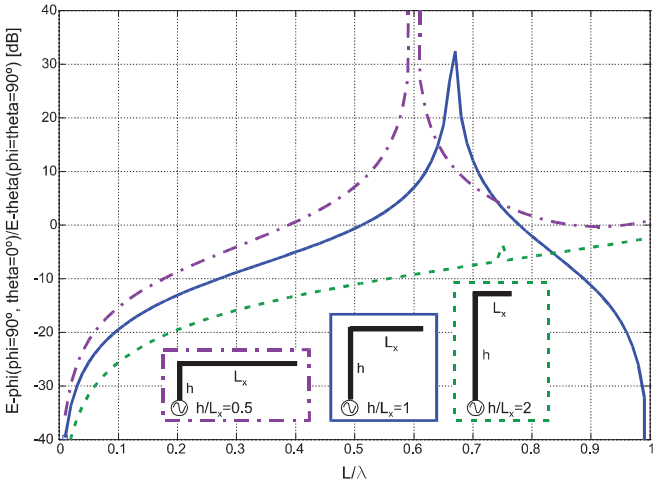

Figure 5. Ratio between component E-φ (Patch direction) and E-θ (Monopole direction) as a L/λ function, when $h/L_x = 2, 1$, and 0.5, regarding a sinusoidal current distribution.

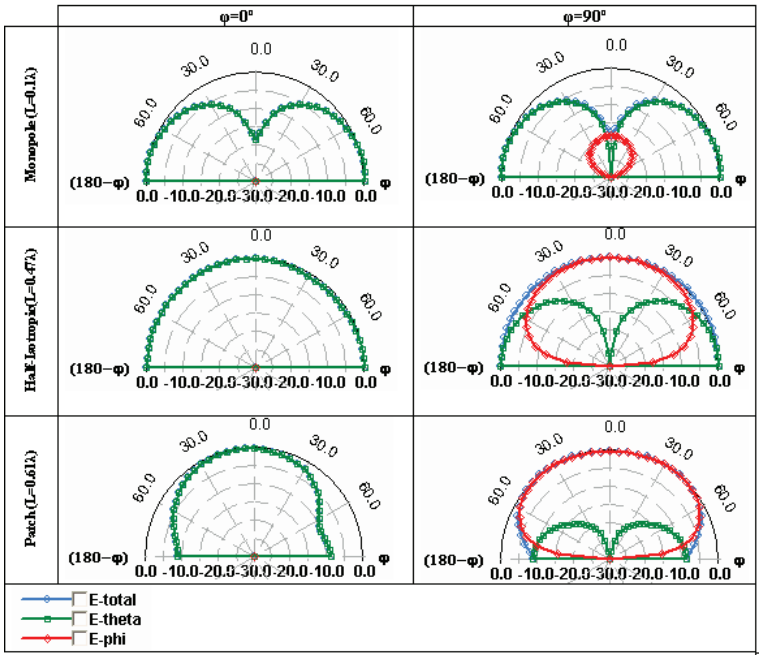

Figure 6. Radiation pattern regarding $h = L_x = 1$ for the most significant $L_{total} = \lambda$ ratios.

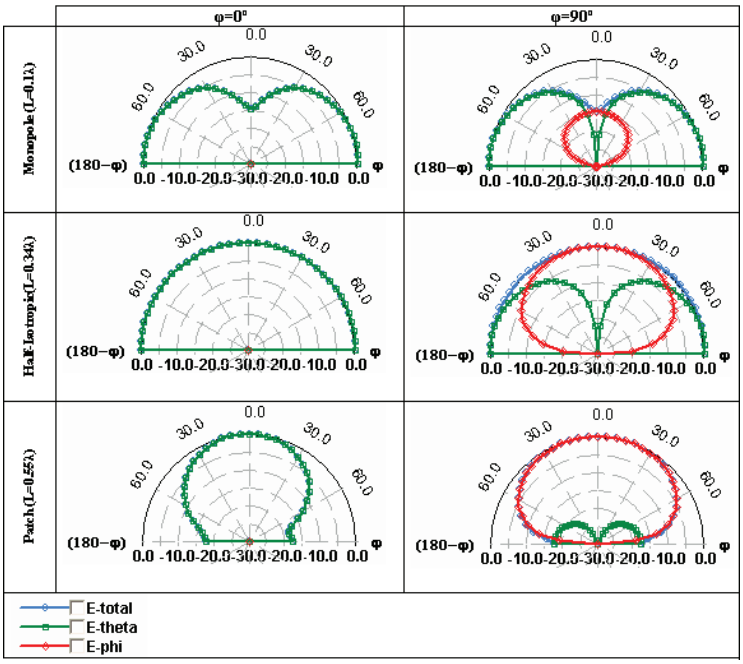

Figure 7. Radiation pattern regarding $h/L_x = 0.5$ for the most significant L_{total}/λ ratios.

4. NUMERICAL RESULTS

In order to test the proposal, an L-shaped wire antenna has been simulated by means of the IE3D MoM simulation software. The radiation patterns are shown in Fig. 6 and Fig. 7. While the left column shows the E-total, E_φ and E_θ for $\varphi = 0°$, the right column shows these values, but now regarding the plane $\theta = 90°$. This representation demonstrates the effectiveness of the proposed method, for determining the radiation pattern of the L-shaped wire antenna, by just knowing the total length of the structure. According to Fig. 5, until the length is approximately 0.5λ the L-shaped wire antenna having $h/L_x = 1$ produces a monopole-type radiation, and at 0.5λ a half-isotropic radiation pattern is attained. Finally, the patch-type radiation pattern is only achieved in a range from approximately 0.5λ to 0.7λ. As a consequence, it is possible to conclude that previous study perfectly matches with the simulated numerical results, becoming the proposal of a good approximation for designing in advance, an L-shaped wire antenna with specific radiation properties.

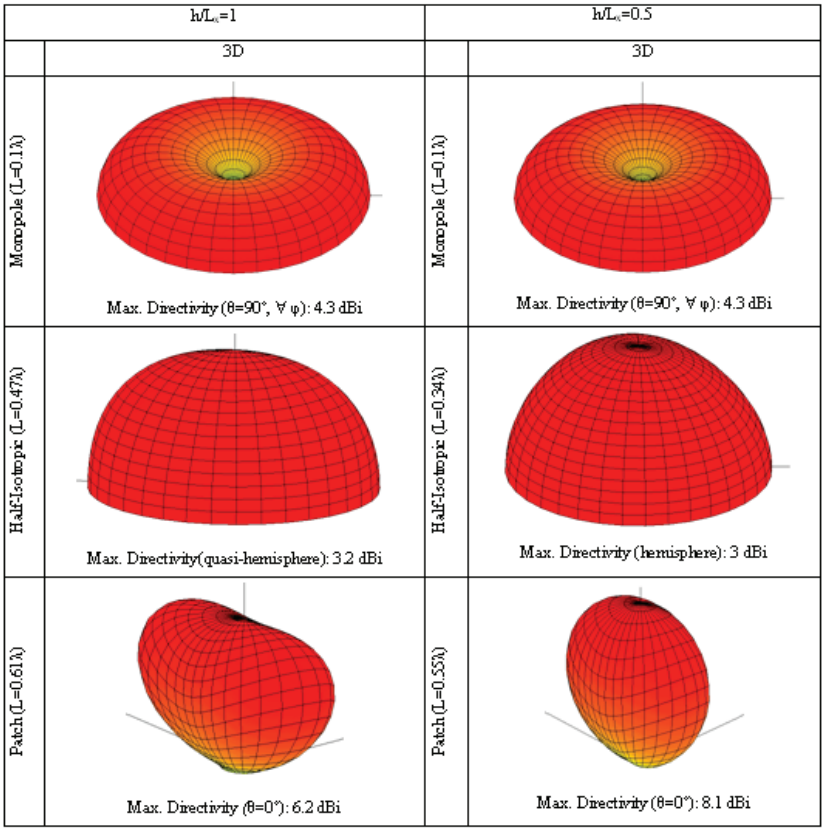

Figure 8. 3D Radiation pattern regarding $h/L_x = 1$ and $h/L_x = 0.5$ for the most significant L_{total}/λ ratios. Dynamic range is 30 dB.

Fig. 7 shows similar results to those of Fig. 6 but for $h/L_x = 0.5$. Again, it is observed the monopole type pattern, half-isotropic pattern (note that is a perfect half-isotropic pattern since directivity is 3 dBi), and finally patch pattern. In this case, the directivity is higher. It should be outlined that other methods can be found in the literature to obtain isotropic patterns such as a combination of monopole and slots [10] or similar techniques consisting in bending the antenna as that presented in [11].

It is interesting to outline that the analytic analysis (Fig. 5) predicts a half-isotropic for 0.5λ ($h/L_x = 1$) and 0.4λ ($h/L_x = 0.5$) while, based on the MoM simulations, they are obtained for 0.47λ (Fig. 6) and 0.34λ (Fig. 7).

The 3D radiation patterns for the cases previously explained are

also shown in Fig. 8. As it is possible to observe the radiation properties of the L-shaped wire antenna are modified insofar the length of the structure in terms of varied λ. The maximum directivity value is determined for the three cases, being maximum when the radiation pattern follows a patch-type pattern.

5. CONCLUSION

A simple method for determining the radiation pattern of an L-shaped antenna structure as a function of length and the ratio between vertical and horizontal arms have been presented. The proposal is focused on obtaining a simplified method, based on the image theory analysis, to easily adapt the radiation properties of a specific structure for the antenna designer necessities. The study demonstrates that it is possible to obtain a patch-type radiation pattern from a monopole-type radiation structure. Not only patch-type radiation pattern may be obtained but also half-isotropic radiation pattern suitable for specific applications such as GPS. At the same time, this concept may be also applicable to control the radiation pattern of a similar radiator, such as a PIFA antenna.

REFERENCES

1. Wunsch, A. D. and S.-P.-Hu, "A closed-form expression for the driving-point impedance of the small inverted L antenna," *IEEE Transactions on Antennas and Propagation*, Vol. 44, No. 2, 236–242, February 1996.
2. King, R., C. W. Harrison, and D. H. Denton, "Transmission-line missile antennas," *IEEE Transactions on Antennas and Propagation*, Vol. 8, No. 1, 88–90, January 1960.
3. Simpson, T. L., "The theory of top-loaded antennas: Integral equations for the currents," *IEEE Transactions on Antennas and Propagation*, Vol. 19, No. 2, 186–190, March 1971.
4. Guertler, R. J. F., "Isotropic transmission line antenna and its toroid-pattern modification," *IEEE Transactions on Antennas and Propagation*, Vol. 25, No. 3, 386–392, May 1997.
5. Hansen, R. C., "Effects of a high-impedance screen on a dipole antenna," *IEEE Antennas and Wireless Propagation Letters*, Vol. 1, 46–49, 2002.
6. Chen, H. T., J. X. Luo, and D. K. Zhang, "An analytic formula of the current distribution for the VLF horizontal wire antenna above

lossy half-space," *Progress In Electromagnetics Research Letters*, Vol. 1, 149–158, 2008.

7. Green, H. E. and J. D. Cashman, "The transmission line antenna revisited," *IEEE Transaction on Antennas and Propagation*, Vol. 38, No. 4, 575–578, April 1990.
8. Balanis, C. A., *Antenna Theory Analysis and Design*, 2nd edition, Chap. 4, 133–203, John Wiley & Sons, 1997.
9. Rogers, S. D., C. M. Butler, and A. Q. Martin, "Design and realization of GA-optimized wire monopole and matching network with 20 : 1 bandwidth," *IEEE Transaction on Antennas and Propagation*, Vol. 51, No. 3, 493–502, March 2003.
10. Long, S. A., "A combination of linear and slot antennas for quasi-isotropic coverage," *IEEE Transaction on Antennas and Propagation*, 572–576, July 1975.
11. Mehdipour, A., H. Aliakbarian, and J. Rashed-Mohassel, "A novel electrically small spherical wire antenna with almost isotropic radiation pattern," *IEEE Antennas and Wireless Propagation Letters*, Vol. 7, 396–399, 2008.